High-performance InP-based Optical Modulators

Takayuki Yamanaka†, Ken Tsuzuki, Nobuhiro Kikuchi, and Hideki Fukano

Abstract

We have developed two types of high-speed semiconductor optical modulators operating at 40 Gbit/s with reduced driving voltage. One is a compact Mach-Zehnder modulator module. The modulator chip has an n-i-n isotype heterostructure for high-speed and low-driving-voltage operation. We obtained error-free operation in a push-pull configuration with a peak-to-peak voltage of 1.3 V. The other is an electroabsorption modulator integrated with microwave coplanar waveguides. A narrow core buried with polyimide provides a steady large extinction ratio and a 3-dB-down frequency as large as 46 GHz. The fabricated modulator operates at a driving voltage as low as 0.79 V.

1. Introduction

The rapid growth of data traffic, caused mainly by increased use of the Internet, has stimulated the demand for high-capacity photonic network systems. High-capacity optical information networks are based on a combination of wavelength division multiplexing (WDM) and high-speed time division multiplexing (TDM) for purposes ranging from long-reach transmission between nodes to short-reach optical links such as metro/access links and intra-office applications. The need for high-speed TDM systems is driving the development of 40-Gbit/s light sources. Semiconductor optical modulators are promising transmitter devices because of their compactness and their ease of monolithic/hybrid integration with laser diodes. In this paper, we focus on two types of semiconductor modulators, namely Mach-Zehnder modulators (MZMs) and electroabsorption modulators (EAMs), which were designed and fabricated using InP-based compound semiconductor technology. The interferometric MZM offers flexibility in increasing the transmission distance through precise chirp control [1] and can generate various modulation formats, including carrier-suppressed return-to-zero (CS-RZ) [2] and return-to-zero differential phase-shift keying (RZ-DPSK) [3]. In addition, unlike a $LiNbO_3$ modulator, a semiconductor-based MZM is free from DC drift. On the other hand, the EAM, which can be monolithically integrated with a distributed feedback (DFB) laser, is expected to be deployed in very-short-reach links because of its ease of operation, administration, and maintenance and its cost-efficiency.

The common issue with these modulators is how to reduce the driving voltage while keeping the bandwidth over 40 GHz. Reducing the driving voltage is a very effective way to reduce the power consumption. Recent progress in Si-Ge technology has made 40-Gbit/s logic ICs possible [4]. A low driving voltage of less than 1 V would enable the integration of logic ICs and driving circuits on one chip using Si-Ge technologies, which would greatly reduce the power consumption, cost, and size of the transmitter module.

This paper describes our recent progress with MZMs and EAMs operating at 40 Gbit/s. For MZMs, we have achieved error-free operation of a push-pull driven module with a reduced driving voltage of 1.3

† NTT Photonics Laboratories
Atsugi-shi, 243-0198 Japan
E-mail: tyama@aecl.ntt.co.jp

V. For EAMs, we have attained error-free operation of a modulator chip with a driving voltage as low as 0.79 V.

2. Push-pull drive MZM module

There are basically two types of conventional semiconductor-based MZM. One is the Schottky electrode modulator [5]. Although a traveling-wave electrode modulator using this structure has been reported to have a bandwidth of over 40 GHz, the relatively wide electrode gap of around 10 µm between the signal and ground electrodes does not provide a strong electric field. So the electrode has to be as long as 10 mm to lower the driving voltage. Moreover, the slow-wave electrode necessary for velocity matching requires very precise control during the modulator fabrication process. The other type of semiconductor-based modulator has a p-i-n structure [6]. This type produces a strong electric field due to an undoped layer with a submicrometer thickness, so the device can be compact. However, the p-type cladding layer induces large electrical and optical signal losses, and the thin undoped layer produces a large capacitance. This makes it difficult to achieve both impedance and velocity matching. Operation at 40 Gbit/s has been reported for p-i-n-type MZMs using capacitively loaded traveling-wave electrodes [1], [7].

We have devised a novel waveguide structure as an alternative way of fabricating a compact MZM with a low driving voltage. The cross section of the waveguide of our novel InP-based traveling-wave electrode MZM is shown in **Fig. 1** [8]. The waveguide is an n-i-n isotype heterostructure grown on a semi-insulating InP substrate. In other words, n-type InP cladding layers are formed on both the signal and ground electrode sides. The low contact resistance and high mobility of these layers contribute to greatly reduce electrical signal loss. In addition, the n-type cladding layers are also beneficial in terms of optical loss. The optical absorption coefficient of n-type InP is more than 20 times smaller than that of p-type InP. The low electrical and optical losses not only enable device operation at a high bit rate but also make it possible to lengthen the phase-shifting region, which leads to a low driving voltage. The 0.2-µm-thick core layer is composed of undoped InGaAlAs/InAlAs multiple quantum well (MQW) layers whose photoluminescence peak wavelength was set to 1.37 µm.

The waveguide also has a semi-insulating InP layer, which performs an electron current blocking role associated with the potential barrier produced by Fe deep levels [9]. An electric field is applied to the waveguide's vertically restricted layers. Therefore, we can obtain an efficient index change induced by the electro-optic effect. The breakdown voltage (i.e., the voltage that induces a catastrophic change in the I-V characteristics) was 15 V, indicating that the current blocking capability of our device is sufficiently high. The deep-etched high mesa buried with benzocyclobutene (BCB) on both sides produces a vertically confined electric field that induces an efficient index change. All waveguide parameters, such as the width of the waveguide and the thickness of the undoped layers and semi-insulating InP layer, are optimized to satisfy the impedance matching and velocity matching requirements.

To reduce the driving voltage and generate zero-chirp optical signals that can accommodate the CS-RZ and RZ-DPSK formats, we devised input and output electrodes for a push-pull driven MZM [10]. The top view of the phase-matched n-i-n MZM is schematically shown in **Fig. 2**. We installed 50-Ω impedance-matched microstrip lines in the input and

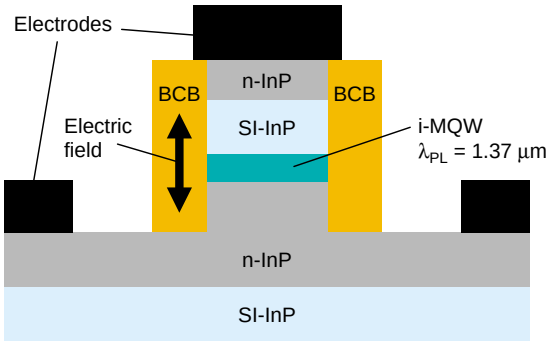

Fig. 1. Schematic cross section of the n-i-n waveguide.

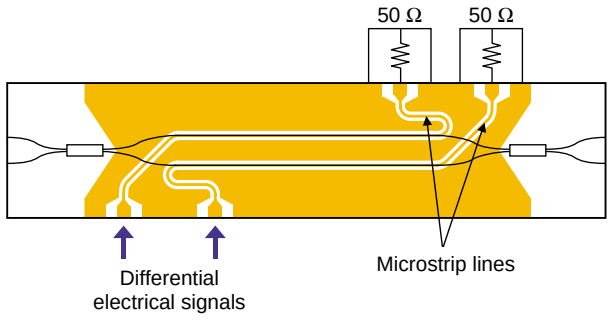

Fig. 2. Schematic top view of the n-i-n MZM with phase-matched dual electrical lines.

output electrodes. The microstrip transmission lines can suppress the electrical loss in spite of the structure's small bending radius. This makes it possible to adjust the length of the dual transmission lines. Consequently, no phase adjustment is required between differential electrical signals. The phase-shifting region is 3 mm long. The device chip size is 4.5 mm × 0.8 mm. The 6-dB bandwidth of electrical S21 is over 40 GHz and S11 stays below –15 dB.

The fabricated modulator was installed in a compact package, as shown in **Fig. 3**. Two RF-input V-connectors for dual driving were placed on one side for ease of connection with the differential output modulator driver. The phase modulation lengths of the dual electrical ports were adjusted to the same value. The package contains 50-Ω terminations and a bias-tee. Its size is 21 mm × 17 mm and it is a conventional butterfly-type with a V-connector mount.

We measured the characteristics of the fabricated module for the entire C-band wavelength range (1.53 µm–1.565 µm). The module had almost the same characteristics as the chip itself, i.e., a DC extinction ratio of more than 20 dB. The π phase voltage was 2.1 V. As shown in **Fig. 4**, the small-signal electro-optical (E/O) 3-dB-down bandwidth was 28 GHz, which is almost the same value as that of the dual ports. Error-free operation was confirmed for a back-to-back configuration with a 40-Gbit/s non-return-to-zero (NRZ) pseudo random bit sequence (PRBS) pulse pattern of a 2^{31}–1 signal, as shown in **Fig. 5**. A driving voltage of 1.3 V_{pp} was supplied to the dual ports of the modulator. No electrical phase adjustment was used for this measurement. The driver outputs were connected directly to the modulator RF ports. The eye diagram obtained for the NRZ 2^{31}–1 PRBS at 40 Gbit/s is shown in the inset of Fig. 5. Clear eye opening was obtained without phase adjustment and the dynamic extinction ratio was 10 dB.

Fig. 3. Photograph of the push-pull drive MZM package.

3. EAM integrated with coplanar waveguides

We designed an EAM having an electrode on the modulator's active part as a microwave-transmission line with both input and output coplanar-waveguide ports on an InP substrate, as shown in **Fig. 6** [11], [12]. The electrode structure of the coplanar wave-

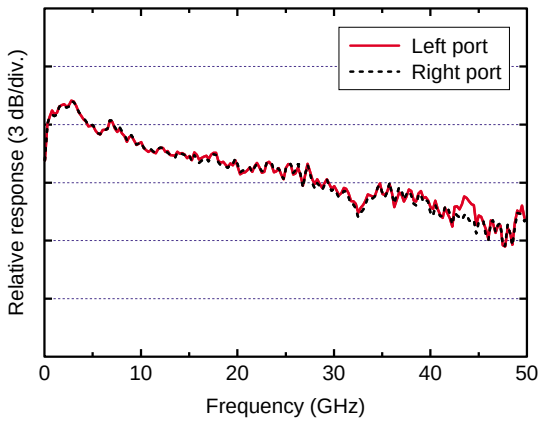

Fig. 4. Small-signal E/O response of the push-pull MZM module.

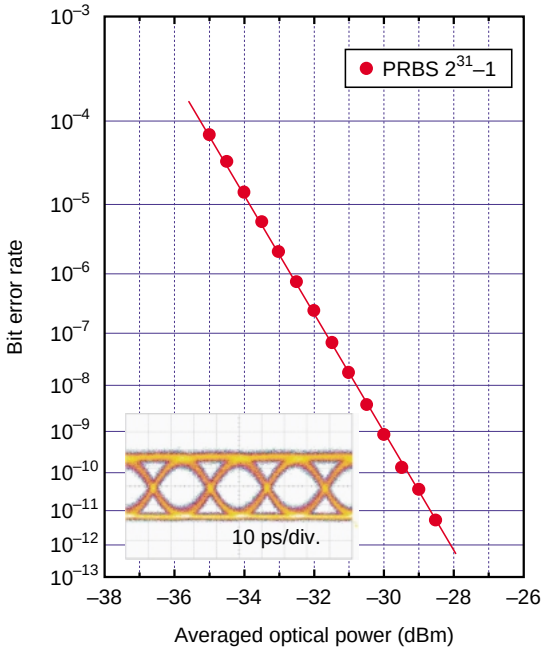

Fig. 5. Measured bit error rate versus averaged optical power for the module in the back-to-back configuration. The inset shows a 40-Gbit/s eye diagram in the push-pull drive configuration with a driving voltage of 1.3 V.

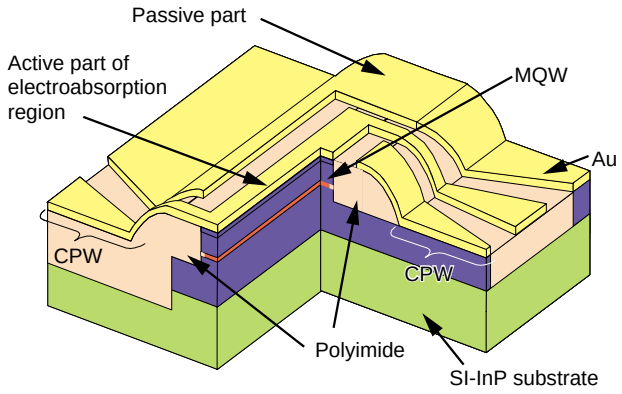

Fig. 6. Schematic view of the EAM integrated with CPWs on SI-InP substrate.

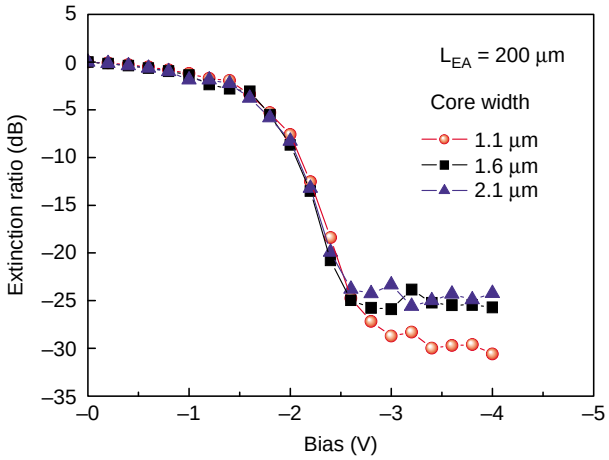

Fig. 7. Relative fiber-to-fiber extinction ratio characteristics for various EA core widths.

guides (CPWs) provides a feed line with a very low microwave-propagation loss. This configuration is superior to the lumped element one in that it minimizes the microwave return loss because there is no significant microwave reflection point. The EAM waveguide has a modulator part incorporating an MQW stack in the p-i-n optical core and passive waveguide parts at both ends.

Our approach to reducing the driving voltage has two aspects. One is the material used for the EAM core and the other is the EAM's structural design. Since InGaAsP MQWs have a small conduction band-gap offset (ΔE_c), the electron state is extended when the applied voltage is high. This results in a weak quantum confined Stark effect (QCSE). However, since InGaAlAs MQWs have a larger ΔE_c, the wells provide stronger carrier confinement. This produces a confined electron state even under a high voltage, resulting in a strong QCSE over a wide range of biases. We used tensile-strained InGaAlAs/InAlAs MQW layers, which show excellent extinction characteristics.

An appropriate structural design provides a larger bandwidth while lowering the microwave loss at the same time. To reduce the driving voltage, we need to increase the extinction ratio and make the slope steep while maintaining the E/O bandwidth required for 40-Gbit/s operation. One simple way to do this is to increase the length of the electroabsorption region. However, when designing the modulator's length, there is a trade-off between the extinction ratio and E/O bandwidth. The best way to relax this trade-off is to make the core narrower in order to enlarge the E/O bandwidth while maintaining strong optical confinement. To obtain strong optical confinement, the mesa must be buried in a low-refractive-index material. For this purpose, we chose to use polyimide. We adjusted the trade-off by optimizing the modulator's stripe width and length. Based on a numerical simulation [13], we confirmed that, even with a 200-µm-long EAM, the combination of an MQW with a large well number of 12 and the narrow core width could provide an E/O bandwidth of more than 40 GHz.

Figure 7 shows the measured relative fiber-to-fiber extinction ratio characteristics for various MQW core widths in a 200-µm-long EAM in the case of 1.55-µm-wavelength TE-polarized light. An extinction ratio of more than 18 dB was obtained even for a voltage swing of only 1 V from –1.5 to –2.5 V. There was almost no degradation in the extinction ratio characteristics even with a core as narrow as 1.1 µm. This is due to the well-designed InGaAlAs/InAlAs MQW core and the strong optical confinement in the core achieved by burying the waveguide with low-refractive-index polyimide. Reducing the width of the EAM waveguide leads to a wider bandwidth because it reduces the p-i-n junction capacitance as well as microwave transmission loss at the p-cladding layer.

The measured E/O responses of 200-µm EAMs for various MQW active core widths are shown in **Fig. 8**. For a 2.1-µm-wide core, the E/O 3-dB-down bandwidth was as small as about 25 GHz. However, as expected, the E/O 3-dB-down bandwidth increased as the core width became narrower and was as large as 46 GHz for a core width of 1.1 µm. This indicates that reducing the core width is a very effective means of increasing the E/O 3-dB-down bandwidth.

Measured 40-Gbit/s driver and optical eye diagrams are shown in **Fig. 9**. Eye opening with a dynamic extinction ratio of 10.5 dB was successfully

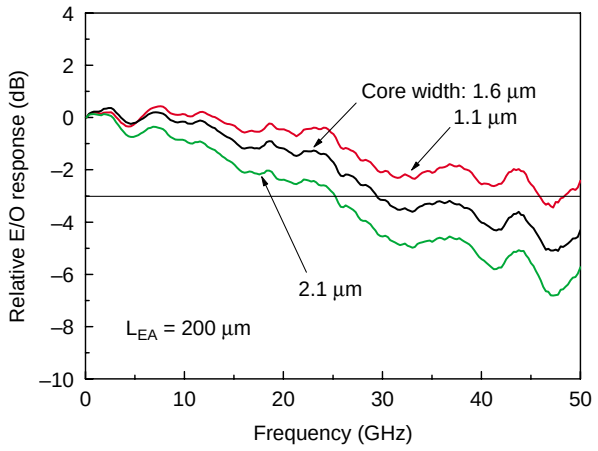

Fig. 8. Small-signal E/O responses of 200-µm EAMs for various core widths.

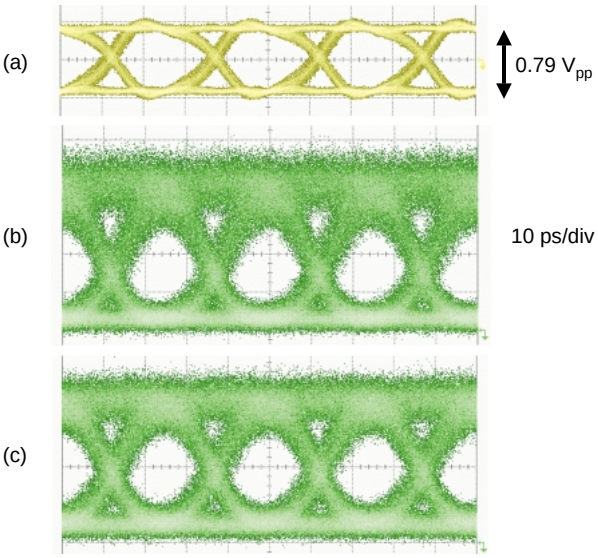

Fig. 9. Measured 40-Gbit/s driver and optical eye diagrams. (a) Driver eye diagram. (b) Optical eye diagram for V_{bias} of –2.2 V. (c) Optical eye diagram for V_{bias} of –2.05 V.

observed even with a peak-to-peak voltage as low as 0.79 V for the device with –2.2-V bias and 50-Ω termination (Fig. 9(b)). Since the on-state side had not sufficiently reached the saturation region of the extinction characteristics for the 0.79-V-swing amplitude of driver voltage, the upper band of the eye pattern signal is large. Somewhat enlarging the swing amplitude or moving the bias point to a low voltage made the swing start from the saturation region and thereby improved the eye pattern. Figure 9(c) shows

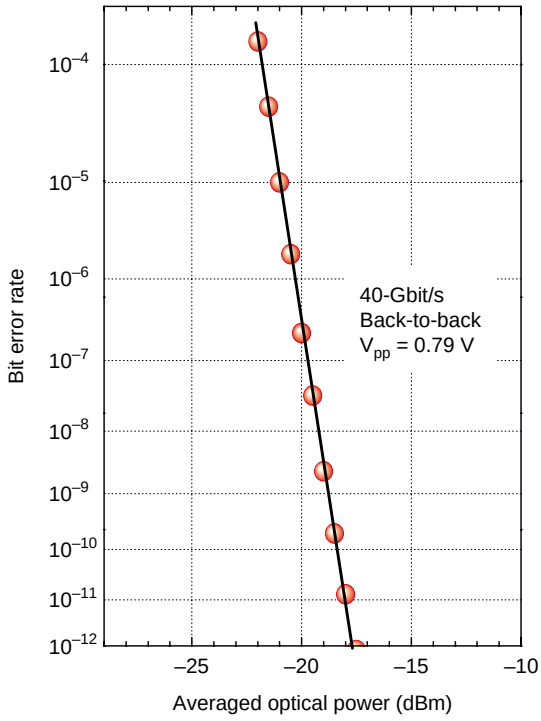

Fig. 10. Measured bit error rate for 40-Gbit/s NRZ signal with 0.79-V driving voltage.

the optical eye diagram of the device for a bias of –2.05 V as an example. Although the upper band is reduced, the extinction ratio is 8.3 dB. We think the main reason for the remaining excess jitter compared with that of the driver signal is the optical axis fluctuation arising from the on-chip measurement using lensed-fiber coupling for both input and output facets. The measured bit error rate for a 40-Gbit/s NRZ PRBS pattern of a 2^7–1 signal with a driving voltage of 0.79 V under –2.2-V bias is shown in **Fig. 10**. Error-free operation was confirmed.

4. Conclusion

We have designed and fabricated high-speed InGaAlAs/InAlAs MZMs and EAMs on semi-insulating InP substrates. A compact packaged MZM with phase-matched dual electrical lines for long-reach transmission systems was developed, and 40-Gbit/s error-free operation at a driving voltage of 1.3 V with a push-pull drive configuration was confirmed. An EAM integrated with coplanar waveguides for very-short-reach links was driven by a voltage as low as 0.79 V. It exhibited an E/O bandwidth of 46 GHz and a dynamic extinction ratio of 10.5 dB.

5. References

[1] S. Akiyama, S. Hirose, H. Itoh, T. Takeuchi, T. Watanabe, S. Sekiguchi, A. Kuramata, and T. Yamamoto, "40 Gb/s InP-based Mach-Zehnder modulator with a driving voltage of 3 V_{pp}," Conference Proceedings of 16th International Conference on Indium Phosphide and Related Materials (IPRM2004), Paper ThA1-4, pp. 581-584, 2004.

[2] Y. Miyamoto, A. Hirano, K. Yonenaga, A. Sano, H. Toba, K. Murata, and O. Mitomi, "320 Gbit/s (8 × 40 Gbit/s) WDM transmission over 367 km with 120 km repeater spacing using carrier-suppressed return-to-zero format," Electronics Lett., Vol. 35, No. 23, pp. 2041-2042, 1999.

[3] A. H. Gnauck, G. Raybon, S. Chandrasekhar, J. Leuthold, C. Doerr, L. Stulz, A. Agarwal, S. Banerjee, D. Grosz, S. Hunsche, A. Kung, A. Marhelyuk, D. Maywar, M. Movassaghi, X. Liu, C. Xu, X. Wai, and D. M. Gill, "2.5 Tb/s (64 × 42.7 Gbit/s) transmission over 40 × ~ 100 km NZDSF using RZ-DPSK format and all-Raman-amplified spans," in Technical Digest of Optical Fiber Communication Conference (OFC2002), post-deadline paper, FC2, 2002.

[4] G. Freeman, M. Meghelli, Y. Kwark, S. Zier, A. Rylyakov, M. A. Sorna, T. Tanji, O. M. Schreiber, K. Walter, J.-S. Rieh, B. Jagannathan, A. Joseph, and S. Subbanna, "40-Gb/s circuits built from a 120-GHz f_T SiGe technology," IEEE J. Solid-State Circuits, Vol. 37, No. 9, pp. 1106-1114, 2002.

[5] R. Spickermann, N. Dagli, and M. G. Peters, "GaAs/AlGaAs electro-optic modulator with bandwidth > 40 GHz," Electron. Lett. Vol. 31, No. 11, pp. 915-916, 1995.

[6] C. Rolland, R. S. Moore, F. Shepherd, and G. Hiller, "10 Gbit/s 1.56 µm multiquantum well InP/InGaAsP Mach-Zehnder optical modulator," Electro. Lett. Vol. 29, No. 5, pp. 471-472, 1993.

[7] R. G. Walker, "High-speed III-V semiconductor intensity modulators," IEEE J. Quantum Electron., Vol. 27, No. 3, pp. 654-667, 1991.

[8] K. Tsuzuki, T. Ishibashi, T. Ito, S. Oku, Y. Shibata, T. Ito, R. Iga, Y. Kondo, and Y. Tohmori, "A 40 Gbit/s InGaAlAs-InAlAs MQW n-i-n Mach-Zehnder modulator with a drive voltage of 2.3 V," IEEE Photon. Technol. Lett., Vol. 17, No. 1, pp. 46-48, 2005.

[9] P. J. Corvini and J. E. Bowers, "Model of trap filling and avalanche breakdown in semi-insulating Fe:InP," J. Appl. Phys., Vol. 82, No. 1, pp. 259-269, 1997.

[10] K. Tsuzuki, H. Kikuchi, E. Yamada, H. Yasaka, and T. Ishibashi, "1.3-V_{pp} push-pull drive InP Mach-Zehnder modulator module for 40 Gbit/s operation," Conference Proceedings of 31st European Conference on Optical Communications (ECOC2005), Paper Th 2.6.3, pp. 905-906, 2005.

[11] H. Fukano, T. Yamanaka, M. Tamura, H. Nakajima, Y. Akage, Y. Kondo, and T. Saitoh, "40 Gbit/s electroabsorption modulators with 1.1 V driving voltage," Electron. Lett., Vol. 40, No. 18, pp. 1144-1166, 2004.

[12] H. Fukano, T. Yamanaka, M. Tamura, and Y. Kondo, "Very-low-driving-voltage electroabsorption modulators operating at 40 Gb/s," J. Lightwave Technol., Vol. 24, No. 5, 2006.

[13] T. Yamanaka, H. Fukano, and T. Saitoh, "Lightwave-microwave unified analysis of electroabsorption modulators integrated with RF coplanar waveguides," IEEE. Photon. Technol. Lett., Vol. 17, No. 12, pp. 2562-2654, 2005.

Takayuki Yamanaka
Senior Research Engineer, Photonic Functional Device Research Group, Photonic Device Laboratory, NTT Photonics Laboratories.
He received the B.E., M.E., and Ph.D. degrees in applied physics from Hokkaido University, Hokkaido, in 1986, 1988, and 1997, respectively. He joined NTT Opto-electronics Laboratories in 1988. Since then, he has been investigating the design and physics of high-speed semiconductor light sources such as distributed feedback laser diodes (DFB-LDs), electroabsorption modulators (EAMs), Mach-Zehnder modulators, and EAM-integrated DFB-LDs (EA-DFBs). He was a visiting scholar at the University of Waterloo and McMaster University, Ontario, Canada, from 1998 to 1999. He is a member of the American Physical Society and the Institute of Electronics, Information and Communication Engineers (IEICE) of Japan.

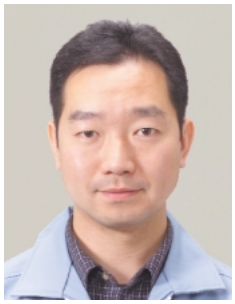

Ken Tsuzuki
Research Engineer, Photonic Functional Device Research Group, Photonic Device Laboratory, NTT Photonics Laboratories.
He received the B.S., M.S., and Ph.D. degrees in applied physics from Tohoku University, Miyagi, in 1993, 1995, and 2005, respectively. He joined NTT Opto-electronics Laboratories in 1995. Since then, he has been engaged in R&D of semiconductor photonic devices for optical fiber communication systems. From 2001 to 2002 he worked at NTT Electronics Corporation. Since 2002, he has been engaged in R&D of semiconductor photonic devices in NTT Photonics Laboratories. He is a member of IEICE and the Japan Society of Applied Physics (JSAP).

Nobuhiro Kikuchi
Photonic Functional Device Research Group, Photonic Device Laboratory, NTT Photonics Laboratories.
He received the B.E. and M.E. degrees in electrical and electronics engineering from Kobe University, Hyogo, in 1995 and 1998, respectively. He joined NTT Opto-electronics Laboratories in 1998. Since 1999, he has been with NTT Photonics Laboratories and is currently engaged in research on optical semiconductor devices and their integrated devices for WDM networks. He is a member of IEICE and JSAP.

Hideki Fukano
Senior Research Engineer, Photonic Functional Device Research Group, Photonic Device Laboratory, NTT Photonics Laboratories.
He received the B.E. and M.E. degrees in electrical and electronic engineering from Toyohashi University of Technology, Aichi, and the Dr.Eng. degree from the Tokyo Institute of Technology, Tokyo, in 1982, 1984, and 1994, respectively. He joined the Atsugi Electrical Communications Laboratories of Nippon Telegraph and Telephone Public Corporation (now NTT) in 1984. Since then, he has been engaged in research on heterojunction bipolar transistors, heterojunction phototransistors, laser diodes, photodiodes, and high-speed receiver optoelectronic integrated circuits based on the InP material system. He is currently researching high-speed electroabsorption modulators (EAMs) and EAM-integrated distributed-feedback lasers. He is a member of IEICE and JSAP.